WING DESIGN FOR DELTA-CANARD CONFIGURATION

W. Kraus
Messerschmitt-Bölkow-Blohm GmbH
Helicopter and Fighter Division
Postfach 801160
D-8000 München-Ottobrunn

Contents

1. Introduction
2. Design Methods
3. Variation of Design Point with Theoretical Method and Verification on Experimental Basis - optimum design -
4. Influence of Instability Margin
5. Drag Reduction by Decambering at Low Lift
6. Leading Edge Droop Gains
7. Influence of Leading Edge Radius
8. Conclusion

1. Introduction

One of the most important tasks is the definition of camber and twist distribution of a wing surface to obtain minimum induced drag throughout the total flight envelope. For a delta canard configuration the complete design must be done by including wing, body and canard. For unstable configuration the possibility to trim the aircraft with positive flap deflections at subsonic speeds and the use of leading edge devices gives additional degrees of freedom for improvement of overall aircraft performance. This report deals with those configurations. The following items are treated:

- A short reference of design methods which are applicable for these configurations is given.
- For 3 slightly different planforms the calculated design in terms of twist and camber for three different design conditions is shown. For these three designs three wind tunnel models were built and tested. Then trimming with trailing edge flaps was done for same trim conditions and drag penalties or gain dependent on design lift coefficient relative to plane wing were evaluated. From this the optimum design lift coefficient can be found, which lies in the order of $c_{Ldes} \sim 0.20$.
- It is shown, that a practicable instability margin of -8% at low lift and low Mach number lies near the aerodynamic optimum for realistic configurations.
- For wings with design lift coefficients greater than $c_{Ldes} = 0.15$ induced drag at low lift coefficients can be reduced by using leading edge flaps up (decambering). This is shown by experimental data for the wing with $c_{Ldes} = 0.20$.
- The results demonstrate that camber drag at 1g flight is not a limiting case for the choice of design c_L, because 50% of the camber drag can be recovered by decambering the leading edge deflecting the L.E. flaps up. The conclusion that for a clean wing a design lift coefficient of $c_{Ldes} = 0.2$ should not be exceeded is not effected by this because decambering only can be used at low lift coefficients. Additional limitations in maximum design lift coefficient might come from the fact that a highly cambered and twisted surface results, which will be difficult for production. Certain local compromises might be necessary.
- Even for the high swept low aspect ratio Delta-type wings leading edge droop can give a remarkable improvement in drag in the sub- and transonic speed regime.
- Blunting the leading edge radius gives remarkable recovery of suction force at low to moderate lift coefficients which results in improvement of induced drag.

The conclusion is a supersonic design for low lift coefficients with moderate instability margin and use of leading edge devices as well for decambering as for conventional droop and of slightly thicker leading edge radii than standard NACA-profiles are giving.

2. Design Methods

The used design method is a simple panel method first published by Woodward [4], further development was done by MBB [5]. The method can handle wing tail or wing canard configurations of arbitrary constellations with fuselage. The only constraint is the restriction to circular body sections. In the method a minimum drag procedure for given lift and pitching moment is incorporated, using the Lagrange multiplier method. Some additional effort was put in smoothing procedures for the integration of the resulting camber slopes and the relationship between wing body setting for the mathematical model with circular body sections and the real configuration [2], [3]. A survey for design methods used at MBB can be found in [1].

3. Variation of Design Point with with Theoretical Method and Verification on Experimental Basis - Optimum Design -

3.1 Planforms

During the last four years several high speed tests with the Conf. 1 wind tunnel model were carried out. The model was fitted with two different wing planforms on the same fuselage with identical canard, fig. 2.

Conf.1 had two wings:

1. $c_{Ldes} = 0$, plane wing (for reference)

2. $c_{Ldes} = 0.12$, $M_{des} = 1.4$ supersonic design.

Conf.3:
$c_{Ldes} = 0.30$, $M_{des} = 0.9$ subsonic design.

A third design was done on a different model, see fig. 3 for an intermediate design lift coefficient and a single engine configuration.

Conf. 1:
$c_{Ldes} = 0.20$, $M_{des} = 0.9$ subsonic design.

This model had a short coupled canard in high position.

A comparison of these three wings, with normalized wingspan, is shown in fig. 1. Configurations are similar, only Conf.2 has a different wing canard arrangement. The following table gives some geometrical data:

	c_{Ldes}	M_{des}	AR	φ	y_{crank}/s	S_{can}/S_{wing}
Conf.1 a.	0.12	1.4	2.27	57°/45°	0.67	0.0816
b.	0.	0.	2.27	57°/45°	0.67	0.0816
Conf.2	0.20	0.9	2.33	54°	-	0.121
Conf.3	0.30	0.9	2.47	57°/45°	0.54	0.0889

3.2 Twist- and Camber Distributions from Theoretical Design

Fig. 4 to 8 show camber and twist for above mentioned three design cases. Camber is compared on 4 spanwise sections:

18%, 46%, 67%, 85%.

Twist for the subsonic design $c_{Ldes} = 0.30$ is remarkable higher than for the supersonic low $c_{Ldes} = 0.12$ design and results in highly cambered surface. The kinks in Conf.2 twist distribution are mainly introduced by the requirement for straight hingelines for L.E. and T.E. flaps, which was not used for Conf.1 and 3, which were not fitted with L.E. flaps.

Looking at the camber distribution in the region of the wing body junction, fig. 5, one can see a very high S-type camber for Conf.2, which is introduced by the short coupled canard in conjunction with the trimming constraint. The comparison for the remaining wing sections shows the right order: increasing c_{Ldes} gives increasing camber heights.

3.3 Trimming Conditions

Trimming should be done for all cases for equal pitching moment characteristics.

All wings have slightly different flap dimensions, fig. 2 and 3, but this will not influence trimmed drag envelopes (see [6]), for different flap sizes only different trim flap angles are necessary.

The main requirement for equal trim characteristics is same zero pitching moment and same stability margin.

Conf.1, 2 and 3 have very similar c_{m0}- and stability behaviour versus Mach number, whereby the zero pitching moment is corrected for same level at Mach number M = 0.5 before trimming and stability margin variation lies in the range of ± 1%. So trim angles of T.E. flap versus c_L are nearly the same, fig. 9, only at M = 1.2 at $c_L = 0$ is a difference which may cause extra trimdrag in addition to the camberdrag.

3.4 K-Factors

So comparison of trimmed drag polars in the dimensionless form of the K-Factor

$$K_{trim} = \frac{C_{Dtrim} - C_{Do}}{C_{L_{trim}}} \cdot \pi \cdot AR,$$

with C_{Do} = zero drag coeff. of the plane wing (no camber drag included)

can give the isolated effect of the influence of the design lift coefficient.

Fig. 10 and 11 show this comparison for sub- (M = .9) and supersonic (M = 1.2) case for all three design cases.

Minimum induced drag factor at Mach number M = 0.9 is reached for $c_{Ldes} = 0.12$ for c_L-values between 0.05 and 0.25, for $c_{Ldes} = 0.20$ between $c_L = 0.25$ and 0.5 and for $c_{Ldes} = 0.30$ between $c_L = 0.5$ and 0.75. This is what was expected, with increasing design lift-coefficient the region where minimum K is reached is increasing.

This region lies higher than the appropriate design lift-coefficient, because due to the benefits of additional camber by trimming with positive flaps the minimum is shifted to higher lift-coefficients. Only for the untrimmed dragpolars with trailing edge flap setting 0° the minimum is in the region of the c_{Ldes}.

For supersonic case, however, the supersonic design (with the lowest design c_L) gives the best values for the whole lift range.

If one takes into account the small improvements in subsonic for higher designs at relative high lift-coefficients in connection with the camber drag penalties at small lift the best compromise seems to be the supersonic design for moderate design lift-coefficients.

3.5 Camber Drag Penalties

To give values for camber drag penalties for the different design lift cases in trimmed condition at low lift coefficients the form of the K-Factor, which is not defined at $c_L = 0$, is not suitable. Therefore in this region the difference to the plane wing is given in form of ΔC_{Di}, based on a common AR = 2.32 for all wings (Fig. 11 ÷ 15).

Due to a lack of test data and for the reason that sub- and supersonic design nearly have the same twist and camber characteristics, in this outline no difference is made between sub- and supersonic design drag penalties.

The data for Conf.1 and Conf.3 fit well on a parabolic curve and even those for Conf.2, which shows configurationwise the largest difference, are lying close to these curves.

From these curves an estimate for the drag penalty depending on design c_L for arbitrary lift coefficients can be done.

As is to be seen, for $c_L = 0$ always a drag penalty is existing, which is nearly independent of Mach number (note:at M = 1.2 there is a trim penalty included, which has to be subtracted for comparison purposes). For increasing c_L one gets more and more a gain in induced drag, which, however, is lost, if design lift-coefficient is chosen too high. An optimum can be found, depending on design lift-coefficient.

3.6 Optimum Design C_L

This is plotted in fig. 16. It is to be seen that design lift-coefficients higher than $c_{Ldes} = 0.20$ are beyond optimum.

Higher camber than for $c_{Ldes} = 0.2$ also produce problems due to the necessity to produce double curvature lines.

4. Influence of Stability Margin

For Conf.1 trimming for three stability margines was done ($c_{Ldes} = 0.12$, $M_{des} = 1.4$). The following reference points with corresponding stability margins were chosen:

$x_{ref}/\bar{c}$	Stab. margin	
0.27	+ 2%	stable
0.35	- 6%	unstable
0.40	- 11%	unstable

This means comparing a conventional configuration (+3%) with a configuration having a sophisticated flight control system (-6%) and a configuration with a flight control system,which is beyond the limit of realization (-11%). The trimming was not simply done for these 3 centers of gravity, it was also taken into account that the configuration should not be limited at C_{Lmax} or somewhere below. To keep the configuration controllable in this region, canard and flaps have to be deflected for flight mechanical reasons away from the position where optimum polar is reached.

This leads to different but realistic schedules for canard and trailing edge flaps for all three cases, see [7]. For higher instability margins therefore the canard at higher A.O.A has to be deflected more negative to relieve the trailing edge flap angular velocity and gives a penalty for higher instabilities which may cancel out part of the advantage. This is to be seen in fig. 17. In supersonic A.O.A. is limited below C_{Lmax}, so the canard can be left in optimum position ($\eta_C = 0°$).

In subsonic the improvement for the most unstable case is not as high as expected and in supersonic for M > 1.4 the best case is -6% instability. The recommendation for this reason is to choose an instability margin of -8%, which simultaneously minimise flight control system problems.

5. Drag Reduction by Decambering at Low Lift

Wind tunnel tests on configuration 2 ($c_{Ldes} = 0.2$), with leading edge droop for decambering ($\delta_{LE\ flap} = -2°$ and $-4°$) were carried out and trimmed. Results are to be seen in fig. 19 and 20. The gain in camber drag at $c_L = 0$ in trimmed condition is even higher than in untrimmed condition. Maximum gain is reached at M = 1.2 and is about 50% of the total camber drag, scaled on camber drag estimates of figs. 12 to 15. This gives a strong indication to use leading edge flaps also for decambering on highly cambered wings.

Trailing edge flaps deflected up certainly gives an improvement in drag in untrimmed condition for small flap angles, fig. 21, trimmed, however, this advantage disappears because of the necessity to trim with the canard, which has less aerodynamic efficiency than the trailing edge flaps, see fig. 22.

6. Leading Edge Droop Gains

For the same configuration as before, also leading edge droop was used to evaluate the gain at higher lift-coefficients, figs. 23 to 24. For a deflection of 25°, this gives a trimmed improvement of 10% to 15% for lift-coefficients higher than c_L = 0.5. With increasing Mach number this advantage is shifted to higher lift coefficients, but the amount of improvement is still higher than at low speeds, which is more or less without explanation, because it is wellknown that the benefit of pure leading edge droop cancels out in the transonic speed regime.

7. Influence of Thickening the Leading Edge Radius

On Conf.1, plane wing case, the influence of a thicker leading edge radius was investigated on the basis of an experimental study. Original and modified profiles are to be seen in fig. 25. The ratio of leading edge radius original to modified is 1:2. The modified profile contour is faired in the original profile contour at the crest (40% chord). An improvement in induced drag by regain of the suction force at the leading edge between 40% and 10%, depending on lift-coefficient and Mach number, fig. 26, is reached. Maximum gains are of course in subsonic for low lift-coefficients.

8. Conclusion

- This report shows on the broad basis of extensive theoretical and experimental work the advantage of supersonic design for moderate design lift-coefficients on delta canard configurations.
- Design should be carried out for the complete configuration, wing and canard in trimmed condition using a drag minimization procedure.
- The optimum instability margin from the aerodynamic side of view seems to be that one, which is attainable from the flight control system.
- Leading edge droop gives remarkable improvements by decambering at the low end of the dragpolar and by conventional use at the high end of the dragpolar.
- Induced drag can be improved remarkable by blunting the leading edge radius.

References

[1] Sacher P., Kraus W., Kunz R., "Computational Aerodynamic Design Tools and Techniques Used at Fighter Development", AGARD Conf.Proc. No. 280 (FMP Neubiberg), 3. - 6. Sept. 1979.

[2] Kraus W., "Wing Design for Delta Canard Configurations - State of the Art - ", TN 173/83 (MBB internal report), 12.4.84.

[3] Schwarze B., "Entwurf des Tragflügels für die Konfiguration TKF J/P mit Hilfe des Woodward/Carmichael Panelverfahrens", AERO-MT-585 (MBB internal report), 2.7.82

[4] Woodward F.A., Tinoco E.N., Larsen J.W., "Analysis and Design of Supersonic Wing-Body Combinations", NASA CR-73106, Aug. 1967

[5] Kraus W., "Ein Computer-Programm zur Berechnung der Druckverteilung und der Beiwerte von Flügeln, Rümpfen, Flügel-Rumpf-Kombinationen und Flügel-Keitwerkskombinationen im Unter-, Über- und Hyperschall", MBB-UFE 1014 (Ö), 13.11.73

[6] Kraus W., "Vergleich der getrimmten induzierten Widerstände anhand der K-Faktoren von 21 verschiedenen Fighter-Konfigurationen", AERO-MT-538 (MBB internal report), 1981.

[7] Haux U., Mayer-Arnold H., "TKF 8.18-10E. Getrimmter Datensatz für $x_s/l\mu$ = 0.27 und 0.40", FE126-46/82 (MBB internal report), 22.10.82.

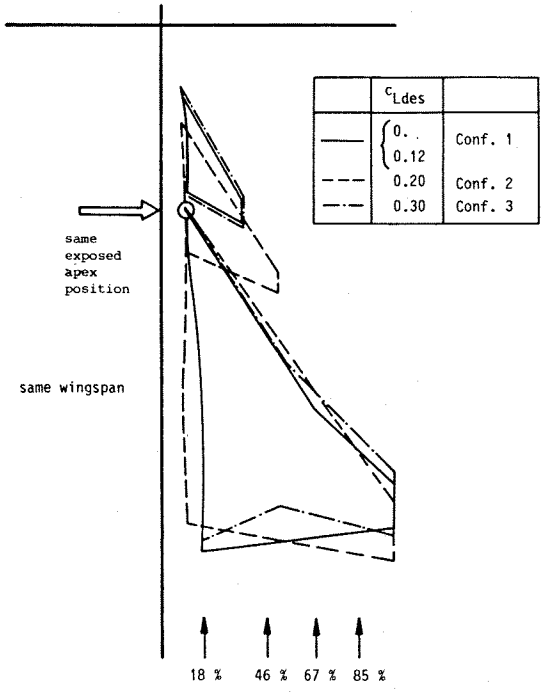

Fig. 1 Wind tunnel models used for variation of design lift coefficient

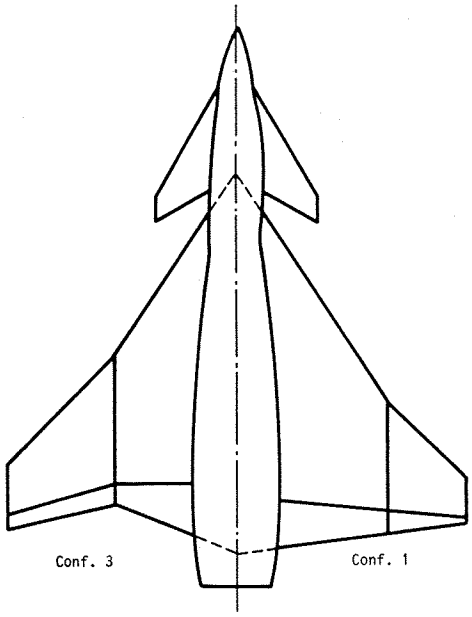

Fig. 2 Wind tunnel models

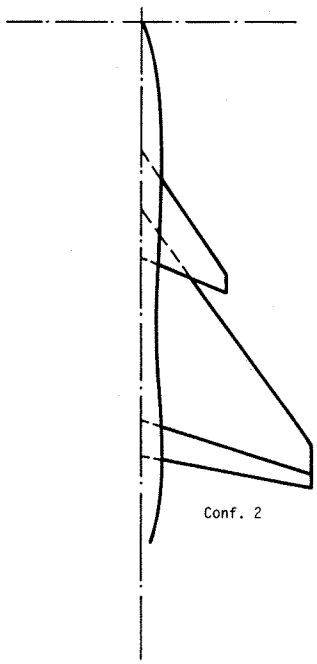

Fig. 3 Wind tunnel models

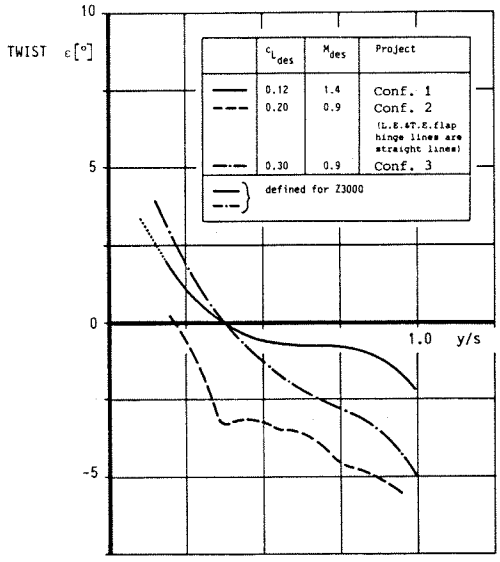

Fig. 4 Twist for the three design cases

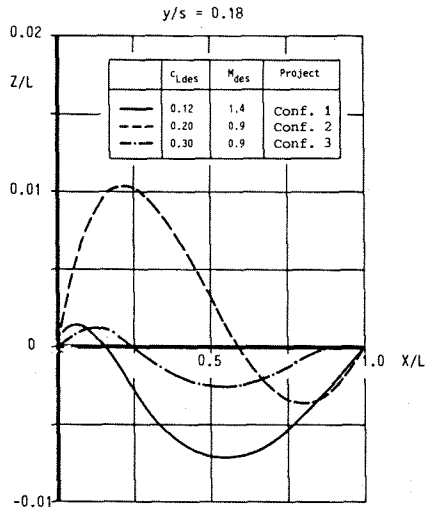

Fig. 5 Camber for the three design cases at y/s = 0.18

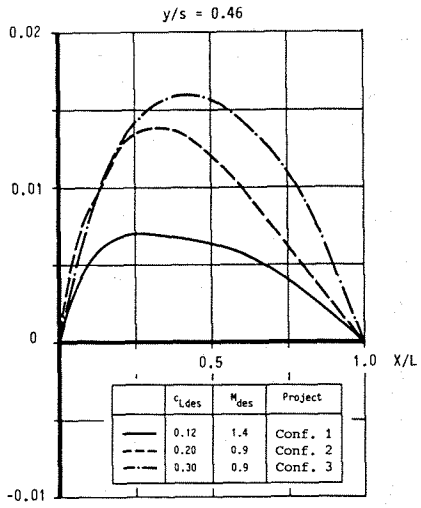

Fig. 6 Camber for the three design cases at y/s = 0.46

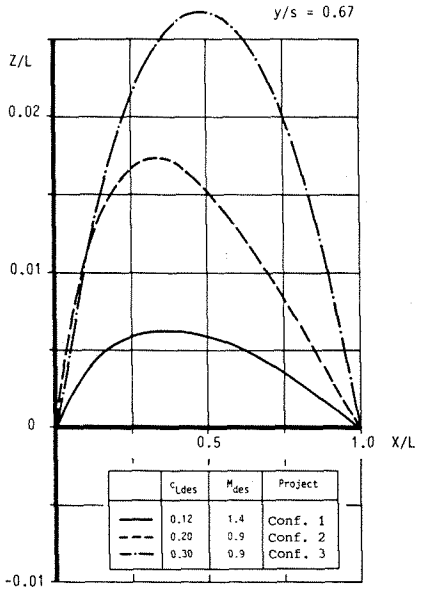

Fig. 7 Camber for the three design cases at y/s = 0.67

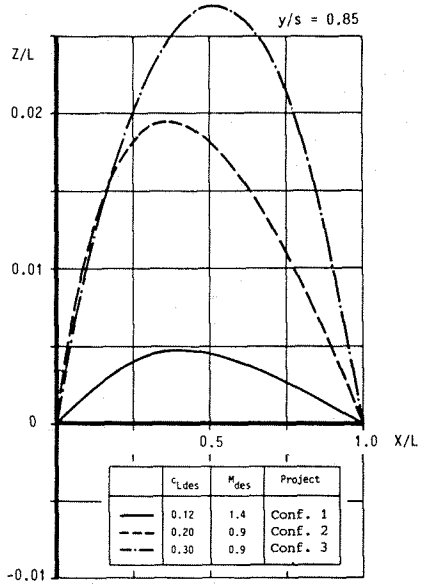

Fig. 8 Camber for the three design cases at y/s = 0.85

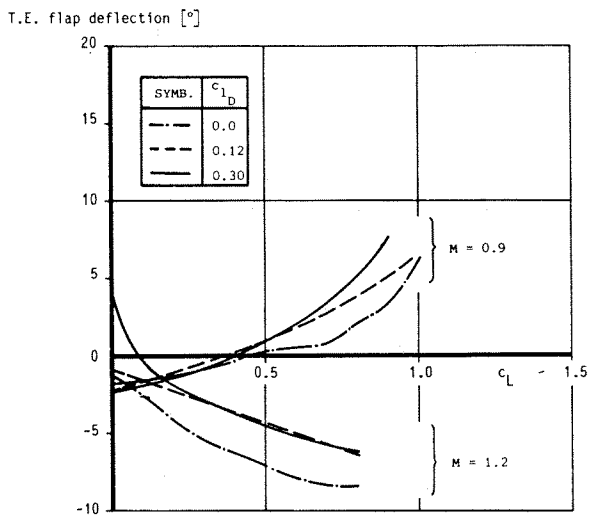

Fig. 9 Trim deflection of t.e. flaps for Conf. 1 and 2

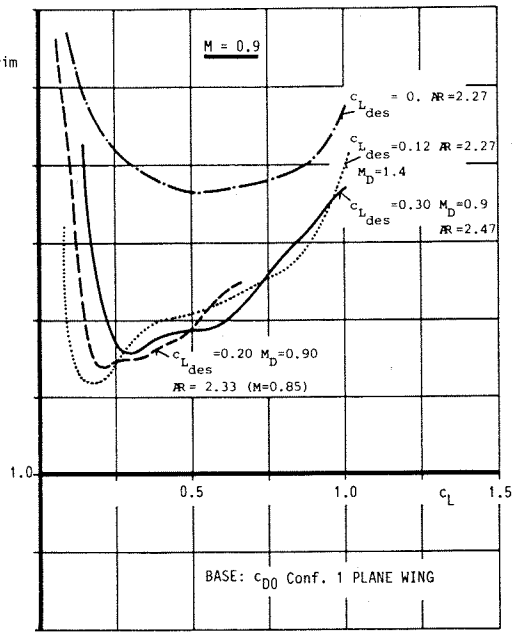

Fig. 10 Trimmed K-factors for all design cases M = 0.9

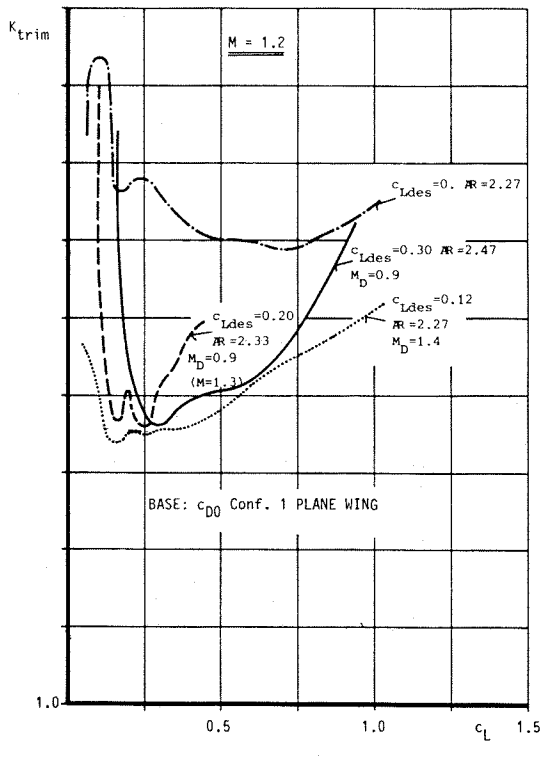

Fig. 11 Trimmed K-factors for all design cases M = 1.2

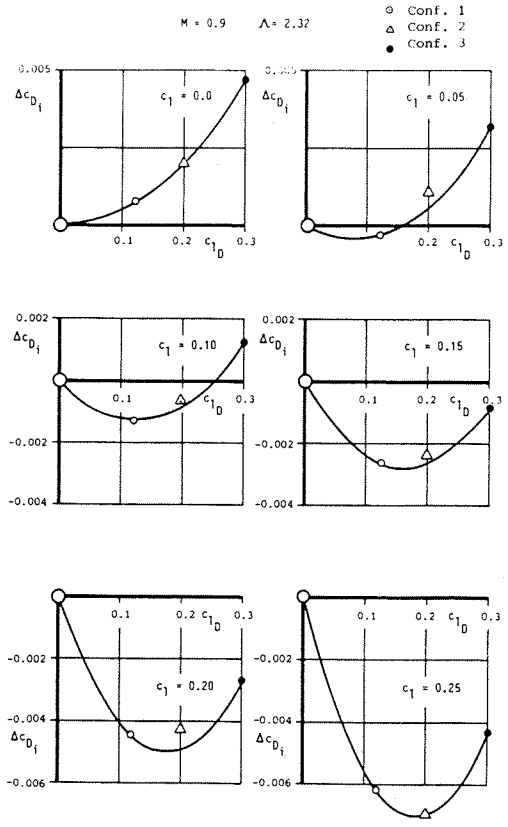

Fig. 12 Drag penalties or gains versus design lift coefficient for the three design cases for several lift coefficients at M = 0.9

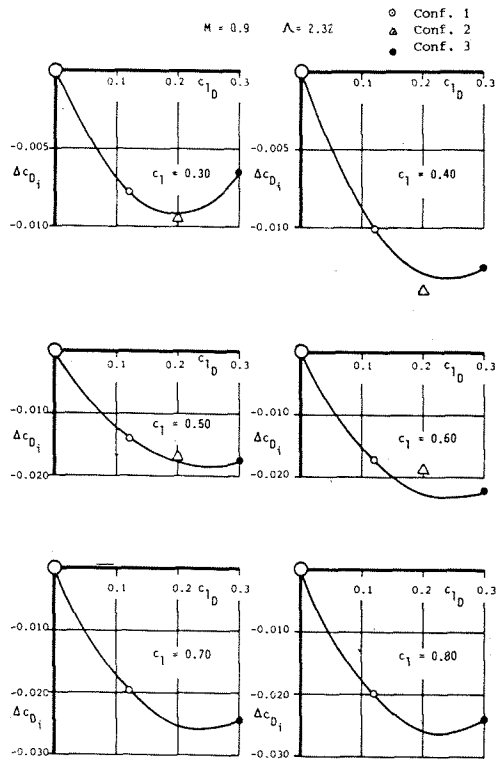

Fig. 13 Drag penalties or gains versus design lift coefficient for the three design cases for several lift coefficients at M = 0.9

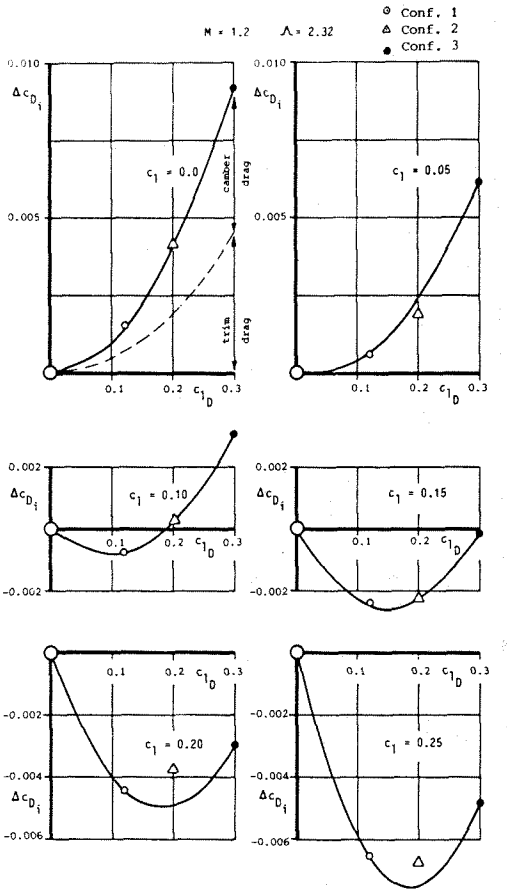

Fig. 14 Drag penalties or gains versus design lift coefficient for the three design cases for several lift coefficients at M = 1.2

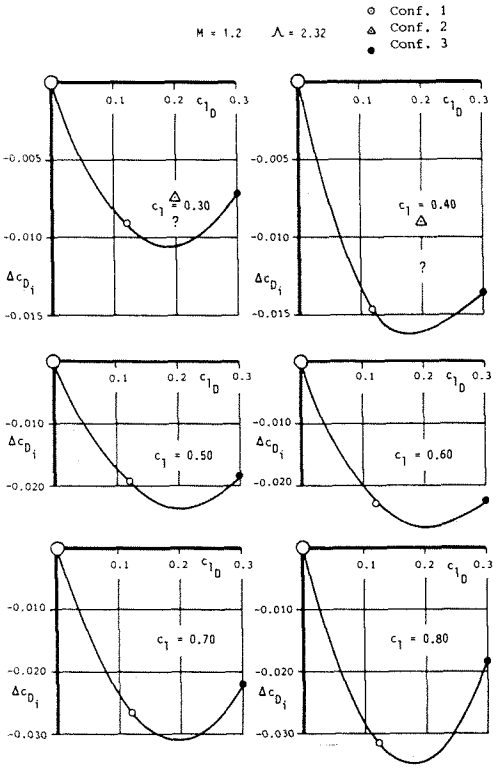

Fig. 15 Drag penalties or gains versus design lift coefficient for the three design cases for several lift coefficients at M = 1.2

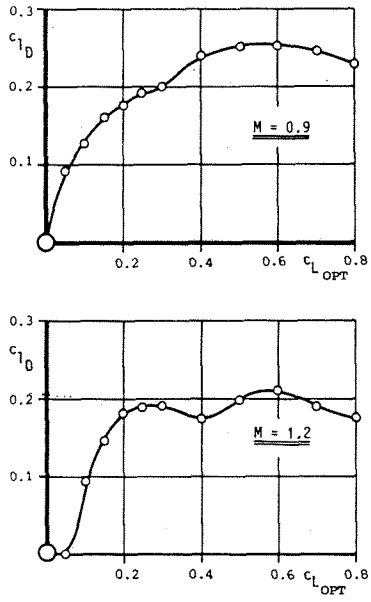

Fig. 16 Optimum design lift coefficient

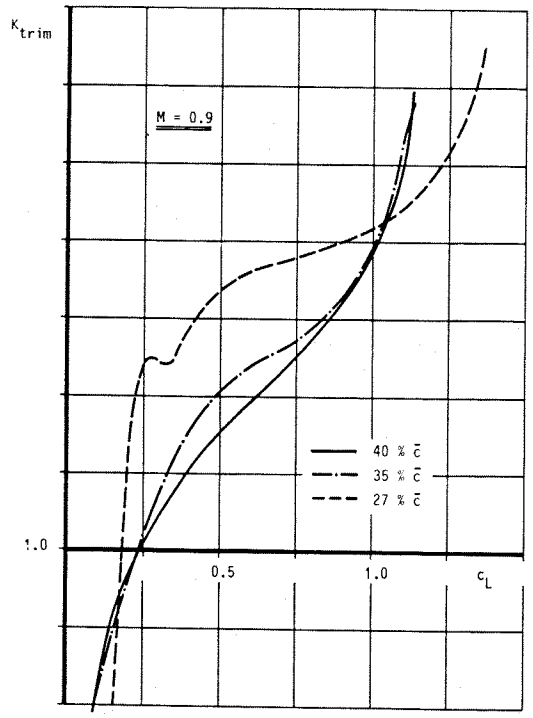

Fig. 17 Influence of stability margin

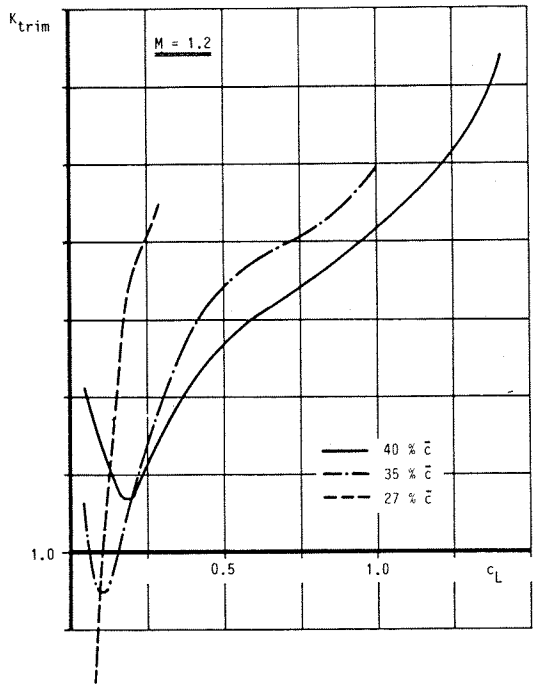

Fig. 18 Influence of stability margin

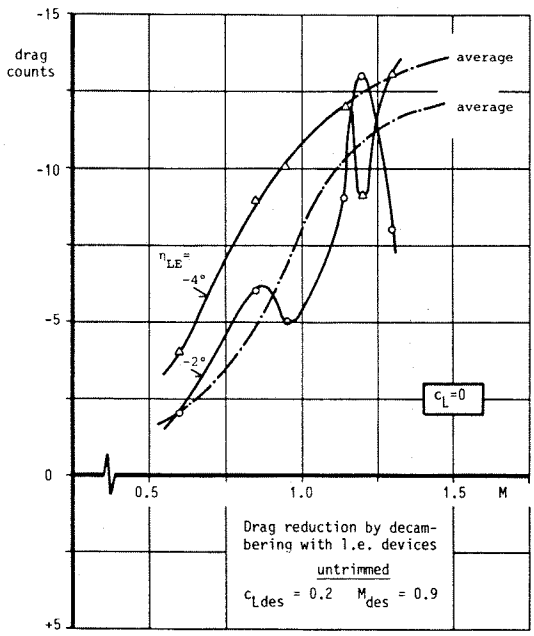

Fig. 19 Drag reduction by decambering with l.e. devices, untrimmed

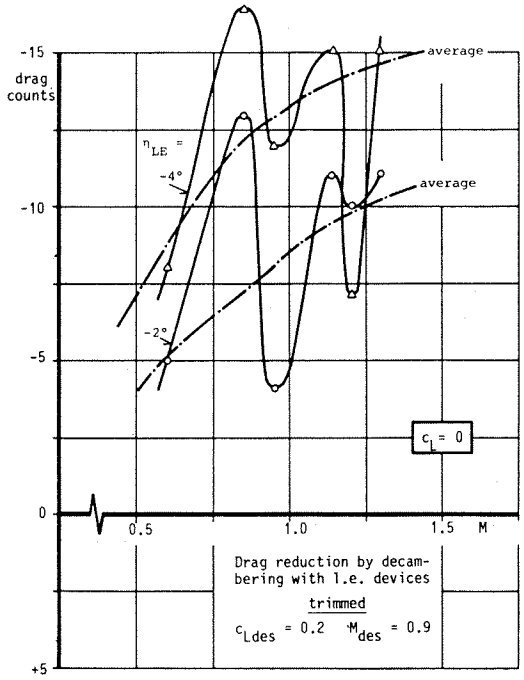

Fig. 20 Drag reduction by decambering with l.e. devices, trimmed

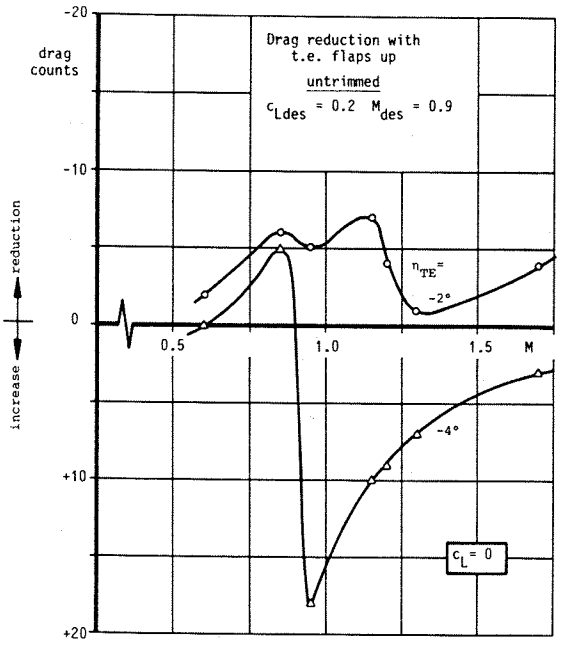

Fig. 21 Drag reduction by decambering with t.e. devices, untrimmed

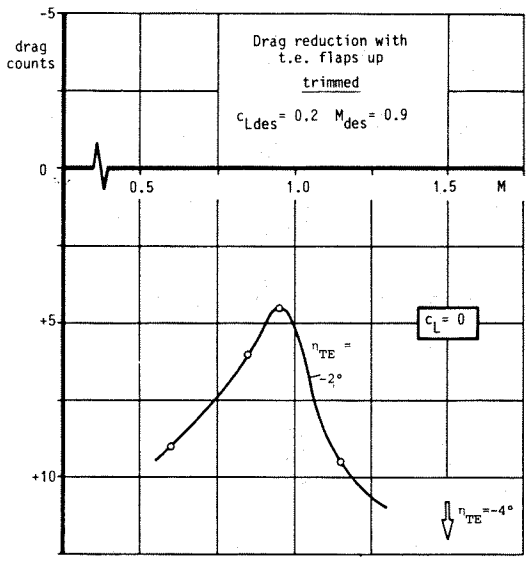

Fig. 22 Drag reduction by decambering with t.e. devices, trimmed

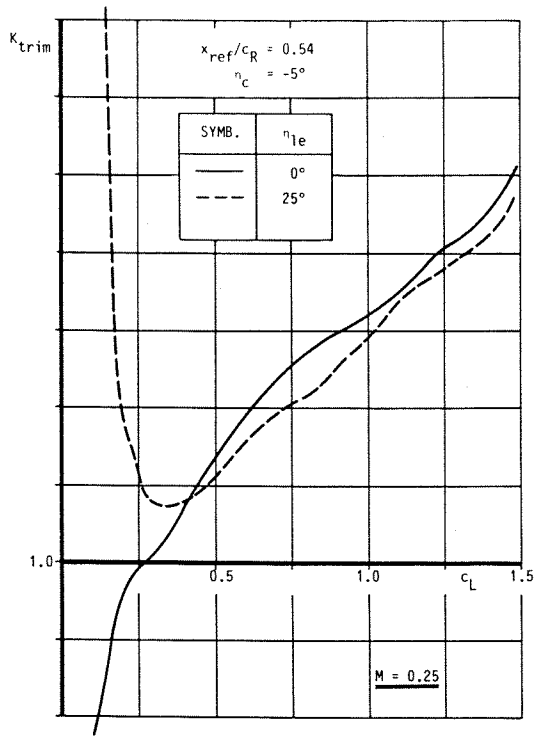

Fig. 23 Leading edge droop gains

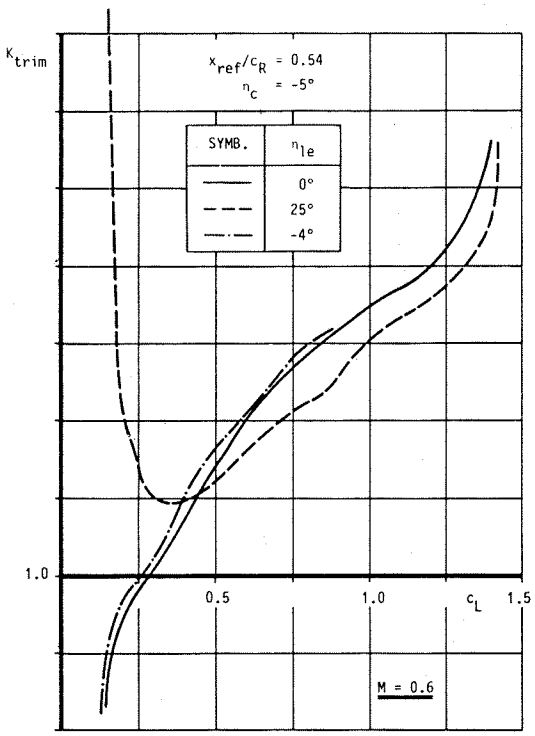

Fig. 24 Leading edge droop gains

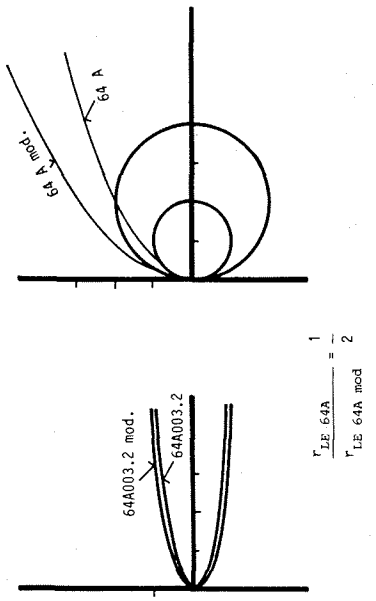

Fig. 25 Influence of thickening the l.e. radius - geometry -

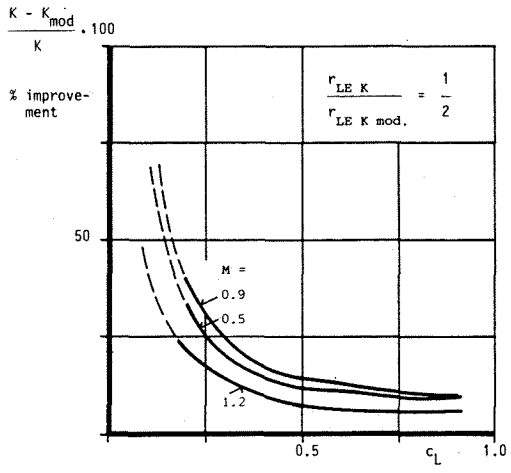

Fig. 26 *Influence of thickening the l.e. radius*
- improvement in percent of trimmed induced drag -